Journal of Radiation and Nuclear Applications
An International Journal

http://dx.doi.org/10.18576/jrna/110104

Health Effects Assessment of Personnel Exposed to Radiation from Background and Scattered Radiation around X-ray Machines at Federal Neuropsychiatric Hospital, Maiduguri

Hamza M. Umar[1], *Ibrahim W. Fawole*[2], *Aliyu Adamu*[2*] *and Atef M. El-Taher*[3]

[1]Department of Physics, Nigerian Defence Academy, Kaduna. Nigeria.
[2]Department of Physics, University of Maiduguri, Nigeria.
[3]Physics Department/ Faculty of Science/ Al-Azhar University/ Assiut/ Egypt.

Received: 30 Aug. 2025, Revised: 20 Oct. 2025, Accepted: 30 Nov. 2025
Published online: 1 Jan. 2026

Abstract: This study presents a comprehensive analysis of radiation exposure levels over 30 days in a medical facility, focusing on six specified locations (R1 to R6). Measurements were consistently taken at an elevation of one meter above sea level using the RADEYE PRD survey meter. The data, expressed in microsieverts per hour (*µSv/hr*), highlights variations in radiation dose rates before and after exposure in the X-ray room, entrance, supervised area, ultrasound room, and at the back of the X-ray room. The overall average dose rates, arranged hierarchically, show R2 with the highest radiation level, averaging 0.1053 *µSv/hr*, attributed to background and scattered radiations inside the X-ray room after exposure. Importantly, all locations exhibit dose rates below the permissible limits set by regulatory bodies. The calculated Annual Effective Dose Rate (AEDR) and Excess Lifetime Cancer Risk (ELTCR) further contribute to the assessment of potential health risks. For instance, R1 has an AEDR of 0.238 *mSv/yr* and an ELTCR of 0.357 *mSv*, demonstrating compliance with international standards.

Keywords: Radiation Exposure, Health Effects, X-ray Machine, Radiation Monitoring, Radiation Protection.

1 Introduction

The interaction between a lepton and a nucleus in an atomic system is typically described by the point-charge Z/r nuclear potential, which assumes the lepton and nucleus are point-like particles [1]. However, this model fails to take into account the finite-size charge distribution of both particles, which arises due to their interaction with external fields, such as the fluctuating vacuum fields. To incorporate these effects, the Z/r potential must be modified, resulting in a perturbation on the Hamiltonian that describes the system [2-4]. To solve for this modified Hamiltonian, various approximation methods have been employed, with time-independent perturbation theory being the most commonly used [5-8]. The first-order perturbation theory is crucial in atomic and nuclear physics, as it allows for the calculation of small changes in lepton energy states due to various effects, including relativistic and spin-orbit effects, nuclear finite-size effects, and effects due to vacuum polarization and fluctuations in the vacuum fields [9-18]. These corrections to the energy levels have paved the way for more precise measurements of fundamental physical constants and the determination of nuclear radii [19-25].

The radiation encountered by humans is diverse in type, energy distribution, and geographical prevalence, with variations related to occupation [1,2]. Human exposure to natural radioactivity is unavoidable, originating from sources like water, soil, plants, food, construction materials, and inhalation of rock and fertilizer dust [3-6]. Additionally, industrial applications, especially in electricity generation and medicine, contribute to continuous radiation exposure [7]. Wilhelm Conrad Rontgen's discovery of X-rays in 1895 revolutionized medical treatment but raised concerns due to their ionizing properties [8,9]. The energy transmitted during X-ray penetration poses risks, potentially leading to the breakdown of biologically significant molecules and the development of cancer [10,11].

Radiology, a crucial diagnostic modality, significantly

*Corresponding author e-mail: aliyuphysics@unimaid.ed.ng

contributes to ionizing radiation exposure in the general population [7]. It is imperative to quantify the radiation exposure from diagnostic X-ray exams to mitigate potential health hazards [12]. X-rays, as man-made ionizing radiations, are widely used in medical settings, can be detrimental to biological systems if precautions are not taken [13,14]. To ensure radiation exposure stays within permissible bounds, it is essential to implement quality control and dosage measurement in medical practices [15,16]. The Nigerian Nuclear Regulatory Authority (NNRA), following the guidelines of the International Commission on Radiological Protection (ICRP), emphasizes maintaining tolerable levels of radiation exposure for nuclear safety and radiological protection (NNRA mandate).

The current study aims to evaluate the radiation dosage received by medical staff in the Radiology Department of Federal Neuropsychiatric Hospital, Maiduguri. The assessment includes background gamma radiation and scattered X-rays, aligning with recommendations from regulatory authorities such as the NNRA, ICRP, and the United Nations Scientific Committee on the Effects of Atomic Radiation. With a focus on radiation safety, the study aims to ensure that individuals are shielded from overexposure to radiation and potential health hazards arising from work-related exposure to ionizing radiation, in line with regulatory guidelines [17].

2 Methodology

The study was carried out at the Federal Neuropsychiatric Hospital, Maiduguri's Radiology Department, which is located in Ibrahim Taiwo Estate on the city's northern outskirts. Latitude 11.8648527º and longitude 13.1191812º are the approximate geographical coordinates, placing it 4.82 kilometers from the city center (Shehu's Palace). The department, which has a CT (Computed Tomography) scan, an ultrasound machine, and a traditional X-ray machine, is about 11.5 meters from the hospital's main door. The X-ray room, which has an XR6000 GE HIGH-POWERED FLOOR-MOUNTED X-RAY MACHINE, was the center of attention for the investigation. This device generates X-ray photons with a quality range of 0.5 *mAs* to 640 *mAs*, operating between 40 *kVP* and 160 *kVP*. The CT room is to the right of the X-ray room, while the ultrasound room is to the left. The fence wall is located about 10 meters from the closest residential homes, and there is a gap of about 1 meter at the back of the X-ray room that leads to it.

Thermo Scientific's RADEYE PRD, a scintillation-based survey meter that is extremely sensitive to gamma and X-ray radiation, was used for the environmental radiation survey. The detector is made consisting of a glass end covered in a semitransparent layer of photosensitive material (photocathode), which is connected optically to a photomultiplier tube via NaI(Tl). Photoelectrons are released from the photocathode when photons interact with it, starting a chain reaction of secondary electron-emitting surfaces called dynos. The quantity of electrons multiplied by this dynode configuration eventually gathers at the anode. In relation to the photocathode, the initial dynode is kept at a positive potential, and subsequent dynodes are positively charged as well. As a result, light pulses are transformed into electrical pulses that may be captured and amplified using the right electronics [18].

The detector was adjusted at the National Institute of Radiation Protection and Research, a branch of the Nigerian Nuclear Regulatory Authority (NNRA), and a Secondary Standard Laboratory approved by the International Atomic Energy Agency (IAEA). This multipurpose pocket meter is very advantageous because of its tiny size, flexibility in operation, convenience of use, and outstanding measuring performance due to its advanced low-power technology. It can also monitor the temperature of its surroundings. Table 1 provides a summary of further information.

Table 1: A detail of the RADEY PRD survey meter.

Parameter	Specification
Detector	NaI(Tl) detector with high-quality micro photomultiplier; software switch for R or Sv energy response and calibration
Measuring Range	1 µR/h - 25 mR/h [0.01 µSv/h – 250 µSv/h]
Over Range Indication	Tested up to 1,000 R/h [10 Sv/h]
Energy Range (± 30%)	60 keV - 1.3 MeV, excellent detection from 30 keV
Response for Cs-137 (662 keV)	1.5 cps per µR/h [150 cps per µSv/h]
Response for Am-241 (60 keV)	30 cps per µR/h [2000 cps per µSv/h]
Linearity Error (Cs-137)	Maximum ± 10%
Enhanced Alarming Sensitivity by NBR	Yes, down to 1 µR/h [0.01 µSv/h] at low gamma energies
Cosmic Radiation Background	Suppression typically > 95%

In order to assess the radiation dose rate at specific locations, the Survey Meter measuring device had to be physically held during the study processes. These locations were used both before and after exposure to X-ray radiation, and they were both within and outside of the X-ray chamber, a controlled area.

3 Results and Discussion

Throughout a consistent period of thirty days, measurements were conducted at a constant elevation of one meter (1 m) above sea level, ensuring the reliability of the dataset outlined in Table 2. The table showcases the documented radiation dose rates at specified locations, employing the RADEYE PRD survey meter, with measurements expressed in microsieverts per hour (µSv/hr). Before exposure, the dose rate within the X-ray room ranged from 0.07 to 0.10 µSv/hr, averaging around 0.0823 µSv/hr. Following exposure, the X-ray room's dose rate fluctuated between 0.09 and 0.12 µSv/hr, with an average of approximately 0.1053 µSv/hr. At the entrance of the X-ray room, the dose rate varied from 0.07 to 0.10 µSv/hr, averaging about 0.0850 µSv/hr. The supervised area 1 meter away from the X-ray room wall showed a dose rate ranging from 0.07 to 0.11 µSv/hr, averaging around 0.0867 µSv/hr. In the ultrasonography room, measured from the X-ray room wall, the dose rate ranged from 0.07 to 0.10 µSv/hr. At the back of the X-ray room, the dose rate varied from 0.08 to 0.13 µSv/hr, with an average of approximately 0.0983 µSv/hr. The calculation of average dose rates using this comprehensive dataset allows for a thorough understanding of radiation exposure levels in the designated locations.

Table 2: The measured radiation dose rates obtained from specific points using the RADEYE PRD survey meter.

Days	Dose Rate *(µSv/hr)*					
	R1	R2	R3	R4	R5	R6
1	0.08	0.10	0.08	0.07	0.08	0.08
2	0.09	0.12	0.08	0.09	0.08	0.10
3	0.08	0.10	0.08	0.10	0.07	0.08
4	0.09	0.09	0.08	0.07	0.08	0.07
5	0.07	0.10	0.09	0.10	0.08	0.09
6	0.08	0.11	0.08	0.09	0.08	0.09
7	0.08	0.10	0.07	0.08	0.09	0.08
8	0.07	0.10	0.07	0.07	0.08	0.08
9	0.08	0.11	0.08	0.08	0.08	0.09
10	0.07	0.10	0.08	0.09	0.08	0.10
11	0.07	0.09	0.08	0.07	0.08	0.09
12	0.07	0.10	0.07	0.08	0.07	0.08
13	0.08	0.10	0.07	0.07	0.08	0.08
14	0.08	0.10	0.08	0.08	0.07	0.08
15	0.08	0.10	0.07	0.07	0.07	0.09
16	0.09	0.11	0.09	0.08	0.08	0.10
17	0.08	0.11	0.09	0.09	0.08	0.11
18	0.09	0.12	0.10	0.10	0.09	0.11
19	0.09	0.12	0.10	0.11	0.10	0.12
20	0.10	0.12	0.10	0.10	0.10	0.12
21	0.09	0.11	0.10	0.09	0.09	0.11
22	0.10	0.11	0.09	0.10	0.10	0.13
23	0.09	0.10	0.09	0.09	0.10	0.12
24	0.09	0.11	0.10	0.10	0.09	0.12
25	0.08	0.11	0.09	0.10	0.10	0.11
26	0.09	0.11	0.09	0.09	0.09	0.11
27	0.08	0.10	0.09	0.09	0.09	0.10
28	0.08	0.10	0.09	0.08	0.09	0.10
29	0.07	0.10	0.08	0.08	0.07	0.10
30	0.08	0.11	0.09	0.09	0.08	0.11

The data in Table 3 reveal the average radiation dose rates recorded over 30 days at different locations (R1 to R6). The arrangement of the overall average dose rates, measured in *µSv/hr* for the 30-day duration, is presented hierarchically as follows:

$$R2(0.1053) > R6(0.0983) > R1(0.0823) > R3(0.0850) > R4(0.0867) > R5(0.0840)$$

This hierarchy signifies the varying levels of radiation exposure at the specified locations. Specifically, the highest level of radiation is observed at R2, where both background and scattered radiation are present inside the X-ray room after exposure. The values indicate the relative magnitude of radiation exposure at each site, with R2 having the highest average dose rate among the measured locations during the 30 days.

Table 3: The average radiation dose rates (ADR) at R1 to R6.

Point	Location Description	ADR *(µSv/hr)*
R1	Inside X-ray room (Background radiation) before exposure	0.0823
R2	Inside the X-ray room after exposure (Background and scattered radiation)	0.1053
R3	Entrance door to the X-ray room	0.0850
R4	Supervised area 1 m away from the wall of the X-ray room	0.0867
R5	Inside the ultrasound room, from the wall of the X-ray room	0.0840
R6	Back of the X-ray room	0.0983

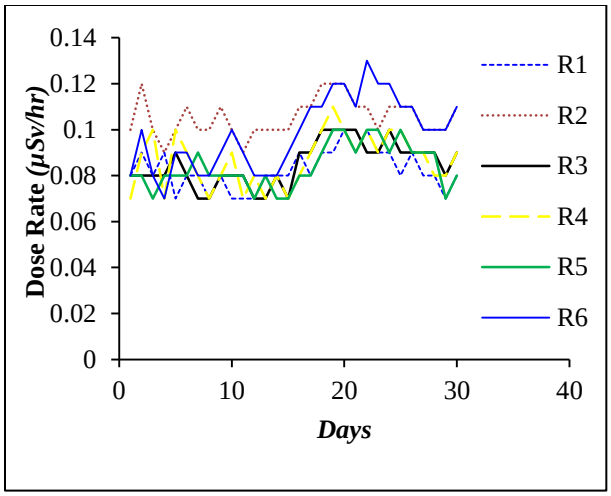

Fig. 1: Variation in the Average Radiation Dose Rate per Day Over 30 days.

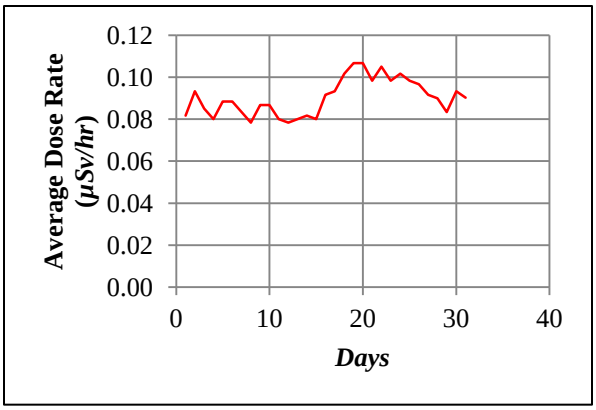

Fig. 2: Variation of ATRDR per Day over 30 days

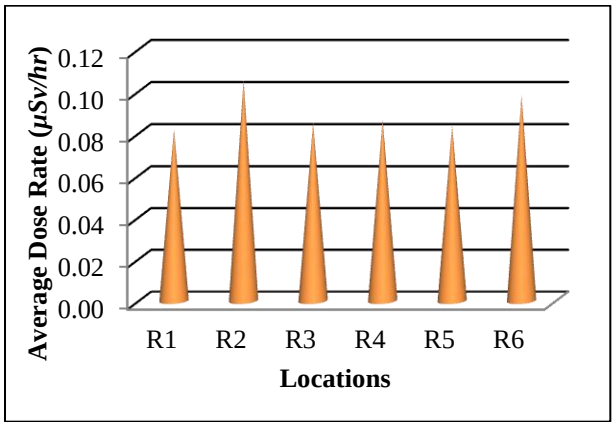

Fig. 3: The average radiation dose rates at R1 to R6

Figure 1 illustrates the fluctuation in the radiation dose rate per day across a 30-day timeframe in each location. The figure serves as a visual representation of the dynamic radiation levels observed throughout the monitoring period, emphasizing days of both heightened and reduced radiation exposure. Figure 2 was plotted to consider the average dose rate in all the locations per day for 30 days. Notably, the plot highlights a peak in radiation levels on the 19th and 20th days, attributed to increased activities during that specific period. Conversely, the 8th day showcases a dip in the average total radiation, possibly reflecting outcomes related to patient-specific factors. Figure 3 presents the average radiation dose rates recorded at different sites (R1 to R6) over 30 days. The data reveal that R2 exhibits the highest radiation dose, followed by R6, R4, R3, and R5, while R1 has the lowest value. This highlights varying radiation levels across different locations, with R2 experiencing the highest radiation, attributed to both background and scattered radiation inside the X-ray room after exposure. Conversely, R1, representing the X-ray room 1 meter away from the X-ray room wall, records the lowest radiation dose. To further assess the potential health impact, the Annual Effective Dose Rate (AEDR) was computed using the following equation:

$$AEDR\ (mSv/yr) = 0.33\left[ADR\left(\frac{\mu Sv/hr}{1000}\right)\left(\frac{8760\ hr}{yr}\right)\right] \quad (1)$$

where the factor 0.33 is an assumed indoor occupancy factor for the personnel. Equation 1 converts the average dose rate (Table 2) into the estimated annual effective dose rate (*mSv/yr*), considering factors such as indoor occupancy. To calculate the excess lifetime cancer risk (ELTCR), the following equation was employed:

$$ELTCR = AEDR \times DL \times RF \quad (2)$$

where DL is the assumed duration of life spent by the medical personnel working in the facility, which is 30 years, and RF is the risk factor of photon radiation as reported by the International Commission on Radiation Protection as 0.05 [19,20]. The outcomes of the calculations utilizing equations (1) and (2) have been intricately outlined in Table 4, shedding light on the cumulative annual radiation exposure at specified locations. Table 5 meticulously displays the computed values of Average Effective Dose Rate (AEDR) for various sensitive body organs. The results of Equivalent Lifetime Cancer Risk (ELTCR) computations, derived from Equation 2, are summarized in Table 4, providing ELTCR values for different sensitive body organs.

Table 4: The values of AEDR and ELTCR from Equation 2 and Equation 3.

Location	AEDR *(mSv/yr)*	ELTCR*(mSv/yr)*
R1	0.238008	0.357012
R2	0.304497	0.456745
R3	0.245718	0.368577
R4	0.250537	0.375805
R5	0.242827	0.364241
R6	0.284261	0.426392

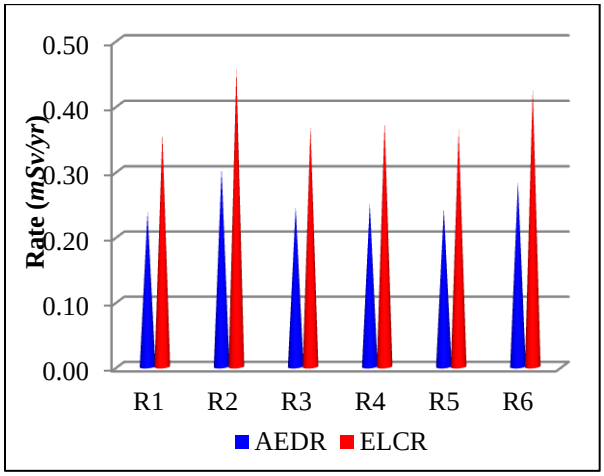

Fig.4: The AEDR and ELCR Exposure Analysis at Different Sites (R1 to R6) Over 30 days.

The presented data in Figure 4 illustrates the values of Average Effective Dose Rate (AEDR) and Excess Lifetime Cancer Risk (ELCR) at various sites (R1 to R6) over a 30-day timeframe. The analysis reveals notable variations in radiation doses across the different locations. R2 consistently exhibits the highest radiation dose for both AEDR and ELCR. This elevated radiation is attributed to a combination of background radiation and scattered radiation within the X-ray room after exposure. The spatial variability in radiation levels is evident, emphasizing the influence of location on radiation exposure. R1, positioned one meter away from the X-ray room wall, records the lowest radiation dose. This suggests effective containment measures, resulting in reduced radiation exposure at this location. The findings underscore the importance of assessing both AEDR and ELCR for comprehensive risk evaluation. Awareness of site-specific radiation levels is crucial for implementing targeted safety measures, particularly in areas with elevated radiation, such as R2. The contrast between R2 and R1 highlights the effectiveness of radiation containment measures, emphasizing the need for continued diligence in maintaining safety standards.

The presented data in Figure 4 elucidates the dynamic nature of radiation exposure across various locations, providing valuable insights for optimizing safety protocols and mitigating potential health risks associated with ionizing radiation.

The Effective Dose Rate of Different Organs (EDRDO) can be determined from the equation:

$$EDRDO = TF \times AEDR \quad (3)$$

where AEDR is the annual effective dose rate and TF is the Tissue-Weighting Factors. From the International Commission on Radiological Protection 103, for skin, it has the value of 0.01; bladder and liver the value is 0.04; while for bone marrow, colon, lungs, and Stomach is 0.12 [20-25]. Additionally, Table 7 showcases the outcomes of Equivalent Dose Rate Due to Organ (EDRDO) calculations using Equation 3, offering insights into the computed values for different sensitive body organs.

Table 5: The computed values of AEDR for different sensitive body organs''.

Location	Annual Effective Dose Rate of Different Body Organs (*mSv/Yr*)						
	Bone Marrow	**Colon**	**Lungs**	**Stomach**	**Skin**	**Liver**	**Bladder**
R1	0.02856	0.02856	0.02856	0.02856	0.00238	0.00952	0.00952
R2	0.03654	0.03654	0.03654	0.03654	0.00305	0.01218	0.01218
R3	0.02948	0.02948	0.02948	0.02948	0.00246	0.00983	0.00983
R4	0.03006	0.03006	0.03006	0.03006	0.00251	0.01002	0.01002
R5	0.02914	0.02914	0.02914	0.02914	0.00243	0.00971	0.00971
R6	0.02584	0.02584	0.02584	0.02584	0.00215	0.00861	0.00861

Table 6: The computed values of ELTCR for different sensitive body organs.

Location	Excess Lifetime Cancer Risk (mSv)						
	Bone Marrow	**Colon**	**Lungs**	**Stomach**	**Skin**	**Liver**	**Bladder**
R1	0.042840	0.042840	0.042840	0.042840	0.003570	0.014280	0.014280
R2	0.054810	0.054810	0.054810	0.054810	0.004575	0.018270	0.018270
R3	0.044220	0.044220	0.044220	0.044220	0.003690	0.014745	0.014745
R4	0.045090	0.045090	0.045090	0.045090	0.003765	0.015030	0.015030
R5	0.043710	0.043710	0.043710	0.043710	0.003645	0.014565	0.014565
R6	0.038760	0.038760	0.038760	0.038760	0.003225	0.012915	0.012915

Table 7: The computed values of EDRDO for different sensitive body organs.

Location	Effective Dose Rate of Different Organs (mSv/Yr)						
	Bone Marrow	**Colon**	**Lungs**	**Stomach**	**Skin**	**Liver**	**Bladder**
R1	0.003427	0.0034272	0.003427	0.003427	0.0000238	0.000381	0.000381
R2	0.004385	0.0043848	0.004385	0.004385	0.0000305	0.000487	0.000487
R3	0.003538	0.0035376	0.003538	0.003538	0.0000246	0.000393	0.000393
R4	0.003607	0.0036072	0.003607	0.003607	0.0000251	0.000401	0.000401
R5	0.003497	0.0034968	0.003497	0.003497	0.0000243	0.000388	0.000388
R6	0.003101	0.0031008	0.003101	0.003101	0.0000215	0.000344	0.000344

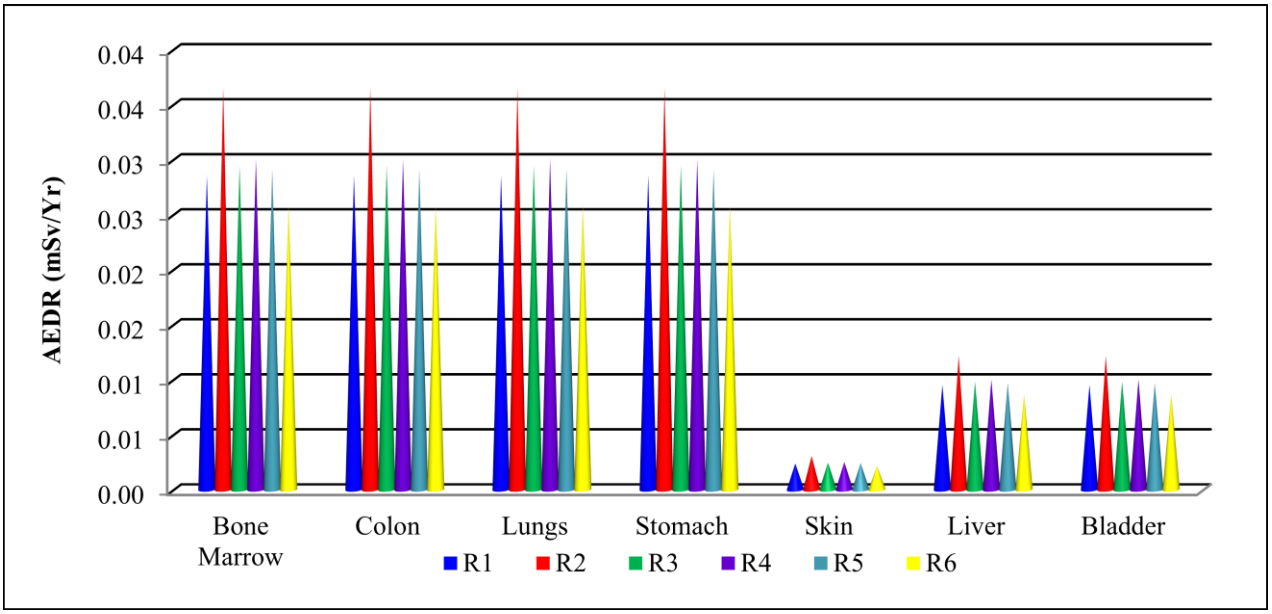

Fig. 5: The values of AEDR for different sensitive body organs.

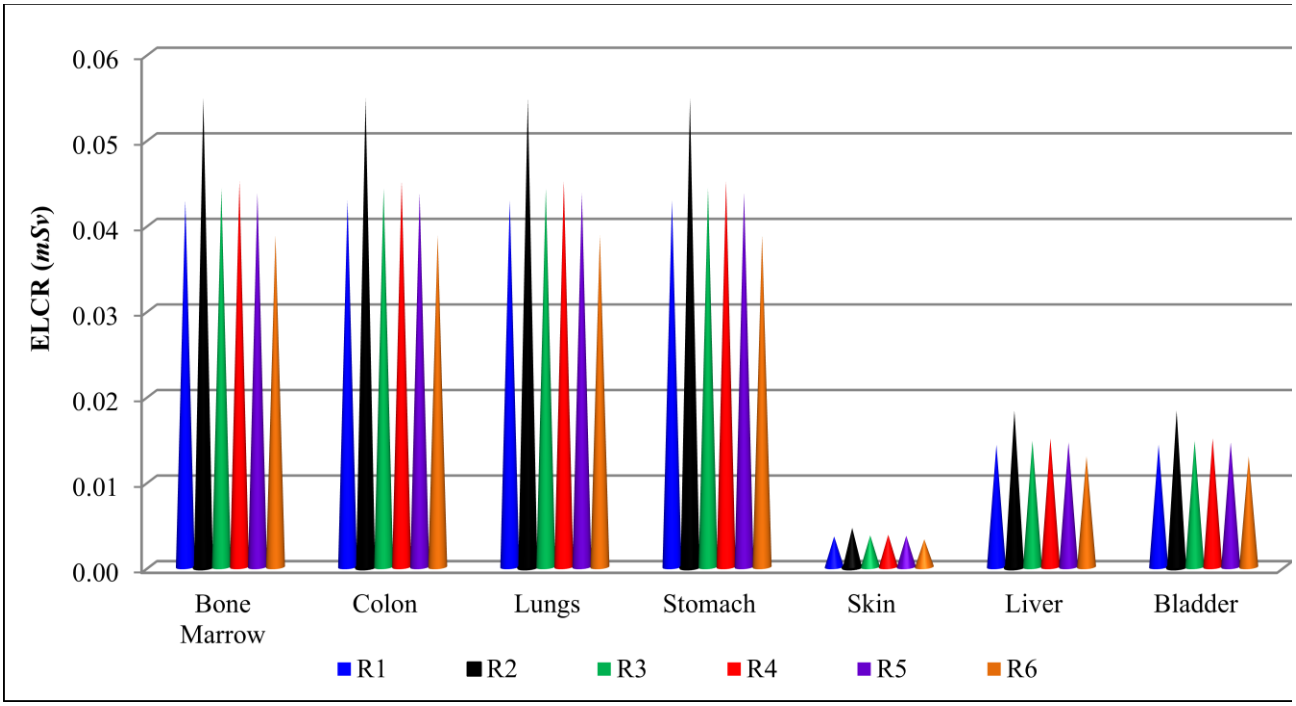

Fig. 6: Excess Lifetime Cancer Risk for different organs.

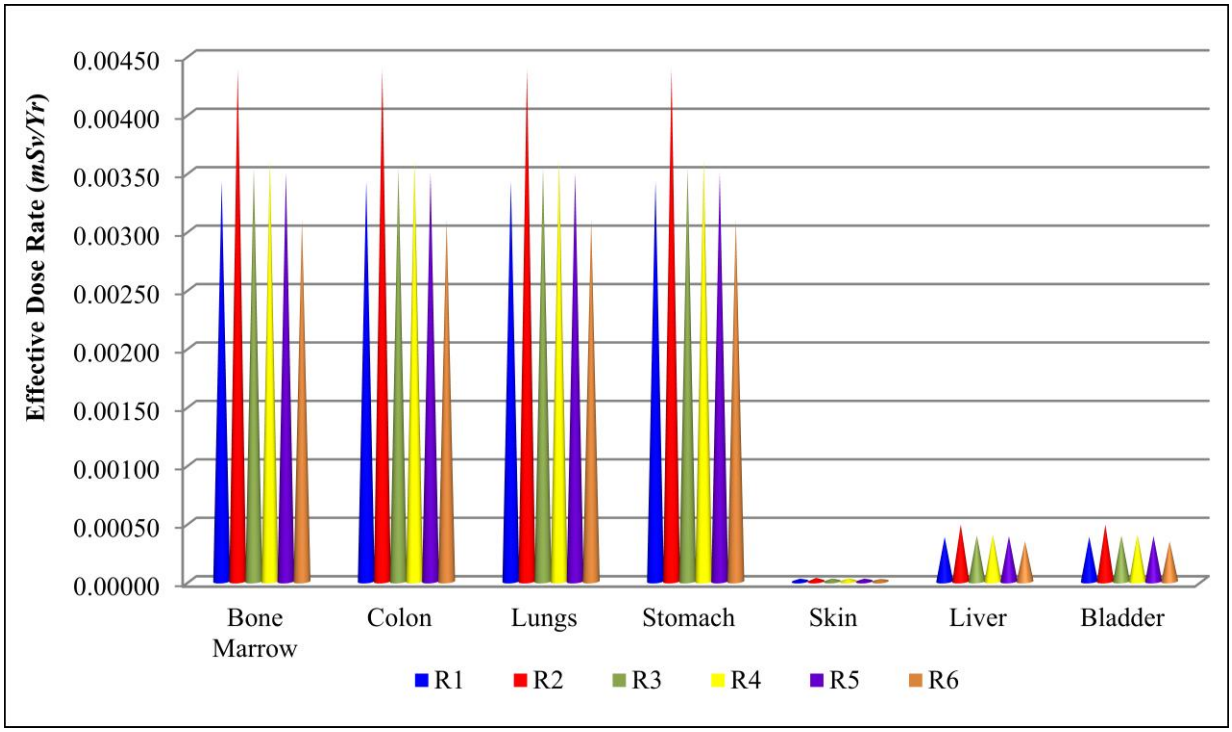

Fig.7: Annual Effective Dose Rate compared with the maximum permissible limit by NNRA and UNSCEAR.

Figure 5 illustrates the AEDR values for different organs, including bone marrow, colon, lungs, stomach, skin, liver, and bladder, as detailed in Table 5. The graph provides a comparative view of AEDR values across multiple organs. The data encompasses locations R1 to R6. All locations (R1 to R6) exhibit AEDR values below the maximum permissible limit specified by the International Commission on Radiological Protection (ICRP).

Figure 6 presents the values representing excess lifetime cancer risks for different organs, as detailed in Table 6. The graph outlines the excess lifetime cancer risk values for bone marrow, colon, lungs, stomach, skin, liver, and bladder. All locations (R1 to R6) show cancer risk values below the maximum permissible limit set by ICRP.

Figure 7 is generated using values computed and presented in Table 7, illustrating the annual effective dose rate for locations R1 to R6. All annual effective dose rate values from R1 to R6 are below the maximum permissible limits specified by the National Nuclear Regulatory Authority (NNRA) and the United Nations Scientific Committee on the Effects of Atomic Radiation (UNSCEAR). Regulatory limits are set at 1 mSv/yr for public exposure and 20 mSv/yr for occupational exposure [26,27]. The positive outcome indicates that the assessed radiation exposure levels align with or are below established safety thresholds, ensuring compliance with regulatory standards. Adherence to the ICRP's threshold for acceptable risk (ELTCR ≤ 1) is observed across all points, indicating that the assessed radiation exposure levels pose a cancer risk within acceptable limits according to international standards [20].

The findings presented in Figures 5, 6, and 7 contribute to the evaluation of potential health risks and affirm the effectiveness of safety measures in maintaining radiation exposure levels within internationally recognized limits. Adherence to regulatory standards and ICRP guidelines underscores a favorable scenario where assessed radiation exposure levels align with or are below established safety thresholds.

4 Conclusions

A 30-day study assessing radiation exposure levels in a medical facility provides valuable insights into potential health risks and safety measures. The highest radiation level was found in R2, aligning with expectations. All locations, maintained dose rates below permissible limits set by regulatory authorities. The calculated Annual Effective Dose Rate and Excess Lifetime Cancer Risk also confirmed overall safety. The findings contribute to ongoing efforts to enhance safety protocols and risk management in medical facilities, ensuring radiation exposure remains within acceptable limits for both public and occupational settings. Furthermore, the study highlights the importance of continuous monitoring and improvement of safety measures to protect individuals from potential health risks associated with radiation exposure.

5 Recommendations

The study on radiation exposure levels in healthcare institutions makes a number of recommendations for enhancing security measures and reducing health hazards. These include keeping an open line of communication with regulatory bodies, conducting regular emergency response training, optimizing structural design for radiation containment, conducting occupational safety training for healthcare personnel, conducting regular monitoring and maintenance of radiation dose rates, making sure radiation detection equipment is calibrated, and conducting periodic reviews of safety practices. These steps are intended to prioritize the health and safety of patients and healthcare providers by promoting a culture of continuous improvement in radiation safety.

References

[1] Smith, F. A. (2000). A Primer in Applied Radiation Physics. World Scientific Publishing Co. Re. Ltd.

[2] Petkoska, T. (2023). Assessment of the Attenuation Properties of Commercial Lead-Free Radiation-Shielding Composite Materials Against Medical X-rays. Journal of Composites Science, 7, 424. https://doi.org/10.3390/jcs7100424.

[3] Josepha, E., Kamal, G., & Bello, O. M. (2023). Natural radionuclide distribution and analysis of associated radiological concerns in rock samples from a rocky town (Dutsin-Ma) in the North-Western region of Nigeria. African Scientific Reports, 2, 125. https://doi.org/10.46481/asr.2023.2.3.125.

[4] Abubakar, S. B., Ibrahim, U., Samson, D. Y., Usman, R., Muhammad, M. I., Nasir, M. A., & Atef, M. E.-T. (2023). Determination of Effective Dose Due to Radon Ingestion and Inhalation from Groundwater Across Awe Local Government Areas in Nasarawa, Nigeria. Rafidain Journal of Science, 32(4), 92-105. https://doi.org/10.33899/rjs.2023.181268.

[5] Nduka, J. K., Umeh, T. C., Kelle, H. I., Ozoagu, P. C., & Okafor, P. C. (2022). Health risk assessment of radiation dose of background radionuclides in quarry soil and uptake by plants in Ezillo-Ishiagu in Ebonyi South-Eastern, Nigeria. Case Studies in Chemical and Environmental Engineering. https://doi.org/10.1016/j.cscee.2022.100269.

[6] El-Taher, A. (2023). BiI3 thick films' structure, linear optical characteristics, and nonlinear optical properties as influenced by the dose of -irradiation for optoelectronics. Conference: The 6 Conference on New Horizons in Basic and Applied Sciences 22-25 September 2023, Hurghada, Egypt At: Hurghada, Egypt.

[7] Najjar, R. (July 10, 2023). Radiology's Ionising Radiation Paradox: Weighing the Indispensable Against the Detrimental in Medical Imaging. Cureus, 15(7), e41623. https://doi.org/10.7759/cureus.41623.

[8] Babagana, U., and Aliyu, A. (2021). Determination of Entrance Surface Dose of Patients Undergoing X-Ray Examination in Federal Neuropsychiatric Hospital, Maiduguri, Nigeria. IOSR Journal of Applied Physics, 13(2), 2278-4861. https://doi.org/10.9790/4861-1302012629.

[9] Kim, E., Park, H., Choi, H., & Ki, J. (2023). An assessment of the usefulness of handheld X-ray devices in general radiography based on a performance evaluation experiment. International Journal of Radiation Research, 21(3), 545-551. https://doi.org/10.52547/ijrr.21.3.26.

[10] Ukerun-Akpesiri, A. A., Akpolile, A. F., Agbajor, G. K., & Mokobia, C. E. (2023). An Assessment of Integrity of Radiation Shielding in X-Ray Radiographic Facilities in Warri Metropolis. FUDMA Journal of Sciences (FJS), 7(5), 1-8. https://doi.org/10.33003/fjs-2023-0705-1897.

[11] Asaad, A. F., Abu Zeid, H. M., Ashry, H. A., Elshahat, Kh. M., William, H., & GabAllah, A. (2023). Evaluation of Image Registry for PET-CT and Image Artifacts and Correction for Radiation Treatment Planning for Cancer Patients (Lung Cancer). Journal of Radiation and Nuclear Applications, 8(2), 113-121. http://dx.doi.org/10.18576/jrna/080202.

[12] Alghoul, A., Abdalla, M. M., & Abubaker, H. M. (2017). Mathematical Evaluation of Entrance Surface Dose (ESD) for Patients Examined by Diagnostic X-rays. Open Access Journal of Science, 1(1), 8–11. https://doi.org/10.15406/oajs.2017.01.00003.

[13] Abuzaid, M. M., Elshami, W., Shawki, M., & Salama, D. (2019). Assessment of compliance with radiation safety and protection at the radiology department. International Journal of Radiation Research, 17(3).

[14] IAEA. (2023). International Atomic Energy Agency. Handbook of Basic Quality Control Tests for Diagnostic Radiology, Human Health Series, No. 47. Vienna.

[15] Langa, E. D., Adamu, A., and Meludu, O. (2020). Occupational Radiation Dose Evaluation in University of Maiduguri Teaching Hospital, Maiduguri, Nigeria. Journal of Radiation and Nuclear Applications, Volume 5, No. 3, pages 181 – 186.

[16] Alechenu, O. J., Umar, I., Akpa, T. C., Mustapha, I. M., Elaigwu, E. D., Chibuike, N. E., & Mundi, A. (2023). Estimation of Diagnostic Reference Level for Chest X-Ray Procedures in Some Radiological Facilities in Abuja Metropolis, Nigeria. Journal of Radiation and Nuclear Applications, 8(1), 59-63. https://doi.org/10.18576/jrna/080109.

[17] Tamam, N., Salah, H., Almogren, K. S., Mahgoub, O., Saeed, M. K., Abdullah, Y., ... Bradley, D. A. (2023). Evaluation of patients' and occupational radiation risk dose during conventional and interventional radiology procedures. Radiation Physics and Chemistry, 207, 110818. https://doi.org/10.1016/j.radphyschem.2023.110818.

[18] Gena, M. A. H., El-Shahat, K. M., Salem, M. Y., Ali, A., & El-Taher, A. (2023). The Influence of Electronic Portal Imaging Devices (EPIDs) used in Radiotherapy: Image Quality and Dose Measurements. Journal of Radiation and Nuclear Applications, 8(3), 237-243. https://doi.org/10. 18576/jrna/080307.

[19] Mustapha, I. M., Fanny, A. U., Adamu, M., Bello, S. M., & Oaniyi, I. W. (2022). Workplace Assessment of Ambient Background Gamma Exposure Level of Some Radiological Facilities in FCT Abuja, Nigeria. Journal of Radiation and Nuclear Applications, 7(3), 27-32. https://doi.org/10. 18576/jrna/070305.

[20] International Commission on Radiological Protection (ICRP). (2007). Annals of the ICRP Publication 103: The 2007 Recommendations of the International Commission on Radiological Protection. Retrieved from https://www.icrp.org/docs/ICRP_Publication_103-Annals_of_the_ICRP_37(2-4)-Free_extract.pdf.

[21] Saleh Alashrah, Sivamany Kandaiya, Nabil Maalej, A. El-Taher., (2014).Skin Dose Measurements Using Radiochromic Films, TLDs, and Ionization Chamber and Comparison with Monte Carlo Simulation. Journal of Radiation Protection Dosimetry, (162) 338-344.

[22] Alsayyari, MAA Omer, Atef El-Taher., (2018). Assessment of Exposure Dose Due to Radioactive Sources at Lab of Radiology Department-Qassim University. Journal of Medical Sciences. 18 (2), 103-107.

[23] Gena Mohamed, KM El-Shahat, M Salem, Atef El-Taher., (2021). Use of Amorphous Silicon (ASi) Electronic Portal Imaging Devices for Other applications for Linear Accelerator Quality Assurance, Iranian Journal of Medical Physics 18 (4), 285-29.

[24] Gena M.A.H , Khalid. M .El-Shahat , , M.Y. Salem and Ahmed Ali , Atef El-Taher ., (2023). The Influence of Electronic Portal Imaging Devices (EPIDs) used in Radiotherapy: Image Quality and Dose Measurements. J. Rad. Nucl. Appl. 8, No. 3, 237-243.

[25] Saleh Alashrah and A. El-Taher., (2015). Intensity-modulated radiation therapy plans verification using a Gaussian convolution kernel to correct the single chamber response function of the I'mRT MatriXX array. Journal of Applied Science, 15(3) 483-491.

[26] NiBIRR. (2020). Nigeria Basic Ionizing Radiation Regulations (Draft). Nigerian Nuclear Regulatory Authority. Third Schedule.

[27] UNSCEAR. (2000). United Nations Scientific Committee on the Effects of Atomic Radiation. Sources and Effects of Ionizing Radiation (Report of the General Assembly). New York: United Nations: UNSCEAR.